Materials International
Open-Access Journal (ISSN: 2668-5728)

Article
Volume 7, Issue 3, 2025, 26
https://doi.org/10.33263/Materials73.026

Green Synthesis and Characterization of *Gelidiella* sp. - Mediated Silver Nanoparticles for Biomedical Applications

A Seethal Papitha [1,*], D Lakshmi [1,*]

[1] Department of Plant Biology and Plant Biotechnology, SDNB Vaishnav College for Women, Chennai- 600044
* Correspondence: seethalpapitha5701@gmail.com (A.S.P.); lakshmisundaram2006@gmail.com (D.L.);
Received: 28.11.2024; Accepted: 4.08.2025; Published: 10.09.2025

Abstract: Silver nanoparticles (AgNPs) were green-synthesized using the aqueous extract of *Gelidiella* sp., red algae. For this 50 mL of 10^{-3} M $AgNO_3$ was prepared and mixed with 50mL of pure *Gelidiella* sp. extract, which was characterized by UV-Vis which had a peak at 417 nm, FTIR which confirmed the presence of functional groups, XRD confirmed the diffraction angles at 2θ=38.2° (111), 44.3° (200), 64.5° (211), 79.6° (311) and 83.3° (331), and SEM analyses which had a particle size ranged from 50 to 60 nm. The silver nanoparticles were evaluated for their antioxidant, antibacterial, and cytotoxic activities. Additionally, the AgNPs demonstrated a strong antioxidant activity via DPPH, Superoxide Dismutase Radical Scavenging assay, $ABTS^+$, Ferric Reducing Antioxidant Potential (FRAP) assay, and Total Antioxidant Activity. Antibacterial tests showed maximal inhibition zones of 24 mm against *Pseudomonas aeruginosa* and *Escherichia coli*. Cytotoxicity analysis on MCF-7 breast cancer cells yielded an IC_{50} of 94.41 µg/mL. Silver nanoparticles synthesized using *Gelidiella offer* an eco-friendly, sustainable method in line with emerging trends in green nanotechnology.

Keywords: *Gelidiella* sp.; silver nanoparticles; antioxidant; antibacterial; cytotoxic activity.

1. Introduction

Algae are abundant organisms rich in proteins, polysaccharides, lipids, and other biomolecules, making them a sustainable resource for nanotechnology. Their natural reducing and stabilizing agents enable environmentally friendly synthesis of nanoparticles, providing a cost-effective, non-toxic alternative to chemical and physical methods for producing nanoscale materials [1,2]. Green synthesis employs algae, fungi, plants, and microorganisms, with natural extracts converting metal ions into nanoparticles through eco-friendly chemical transformations [3-6]. This eco-friendly approach yields nanoparticles that are effective and safe for human health and the environment. Among biosynthesized nanomaterials, particularly silver and gold nanoparticles stand out for their biocompatibility, low toxicity, and broad biomedical applications, including drug delivery and diagnostics [7,8].

Recent studies [9] highlight marine algae's rising prominence in nanomedicine, especially for the facile synthesis of nanoparticles showing enhanced therapeutic effects.

The genus *Gelidiella*, a red alga from tropical regions, is rich in phenolics, flavonoids, and sulfated polysaccharides- compounds that enhance its potential for nanoparticle synthesis and biomedical use. Prior studies demonstrate that *Gelidiella acerosa* can synthesize silver

nanoparticles with strong antimicrobial activity against pathogens such as *Staphylococcus aureus*, *Escherichia coli* [10]. Breast cancer persists as a leading cause of cancer mortality among women worldwide. While conventional treatments include surgery, radiation, and chemotherapy, recent advances in nanotechnology suggest using green-synthesized silver nanoparticles (AgNPs) as adjuncts to improve therapeutic outcomes and mitigate side effects [11,12]. This study evaluates the ability of *Gelidiella*-mediated AgNPs to exhibit combined antioxidant and cytotoxic potential, establishing correlations between their structural parameters and biological activities. The study uniquely demonstrates the comprehensive biomedical potential of *Gelidiella*-derived silver nanoparticles by integrating structural characterization with antioxidant, antibacterial, and anticancer evaluations in an integrative approach. The seaweed was characterized using UV-Vis spectroscopy, Fourier Transform Infrared Spectroscopy (FTIR), X-ray Diffraction (XRD), and Scanning Electron Microscopy (SEM). Antioxidant activity was assessed by DPPH, Superoxide Dismutase Radical Scavenging assay, ABTS Radical Cation Scavenging assay, FRAP, and total antioxidant activity. Antibacterial effects were tested against both Gram-positive (*Bacillus subtilis*, *Staphylococcus aureus)* and Gram-negative (*Escherichia coli*, *Pseudomonas aeruginosa*) bacteria, while cytotoxicity was analyzed using the MTT assay on MCF-7 cells. Compared to existing reports, only limited studies have explored the systematic correlation of *Gelidiella* sp.-mediated AgNPs structure and targeted biomedical properties. This work advocated further research into *Gelidiella*'s bioactive metabolites and their molecular mechanisms against cancer.

2. Materials and Methods

2.1. Chemicals and reagents.

The chemicals used were Silver nitrate ($AgNO_3$ ≥99% purity, analytical grade), 1,2-diphenyl-2-picryl-hydrazine radical (DPPH), and 2,20-azinobis-3-ethylbenzothiazoline-6-sulfonic acid (ABTS), which were purchased from SRL Chemicals Pvt. Ltd, ferrous sulfate ($FeSO_4 \cdot 7H_2O$, ≥98% purity), potassium persulfate ($K_2S_2O_8$, ≥99% purity), methanol (CH_3OH, ≥ 99.8% purity), ethanol (C_2H_5OH, ≥99.9% purity, absolute), and sodium hydroxide (NaOH, 0.1M). All chemicals used were of analytical grade and used without further purification. Double-distilled water was used throughout the study for solution preparation. DPPH and ABTS solutions were prepared using methanol (analytical grade, purchased from SRL chemicals).

2.2. Collection of samples and extract preparation.

Gelidiella sp. were collected fresh from the Rameshwaram coast, Tamil Nadu, in October (available in the post-monsoon season from August to January). Taxonomic identification was confirmed through morphological and anatomical characteristics using standard phycological keys and herbarium references. Samples were washed with tap water, then with sterile distilled water, shade-dried at room temperature for 4-5 days, and ground to a fine powder. One gram of powder was boiled in 100 mL of distilled water for 15 min, cooled, filtered, and stored for further use.

2.3. Synthesis of silver nanoparticles at room temperature.

Silver nanoparticles were synthesized by mixing equal volumes of freshly prepared 1 mM $AgNO_3$ solution and *Gelidiella* sp. aqueous extract. The reaction mixture pH was adjusted to 9.0 with 0.1M NaOH, a value previously shown to enhance nanoparticle formation and stability by promoting efficient bioreduction and minimizing aggregation. The synthesis was conducted at room temperature, a condition suitable for green methods and that avoids unwanted thermal degradation of bioactive compounds. The reaction was allowed to proceed for 24 hours to ensure complete reduction, as monitored by a color change indicating nanoparticle formation. After incubation, the nanoparticles were collected by evaporation and dried at 105°C [13]. The quantitative yield was determined by weighing dried nanoparticles:

Equation 1

$$Yield\ (\%) = (Mass\ of\ dried\ AgNPs/\ total\ initial\ AgNO3\ mass) \times 100.$$

To confirm the bioreduction mechanism, a blank control reaction was conducted by mixing 1mM $AgNO_3$ with distilled water instead of algal extract under identical conditions. Lack of nanoparticle formation in the control validated that bioreduction was mediated by *Gelidiella* sp., biomolecules.

2.4. Characterization of synthesized Ag nanoparticles.

UV-vis absorption spectra were recorded using a Shimadzu UV-1800 spectrophotometer, from 200 to 800 nm with high resolution. FTIR spectra were obtained by a PerkinElmer Spectrum Two spectrometer in the 4000–400 cm^{-1} range at 4 cm^{-1} resolution. X-ray diffraction (XRD) was performed on a Rigaku diffractometer with Cu-Kα radiation (λ = 1.5406 Å), operating at 40 kV and 30 mA, with a scanning range of 5° to 80° 2θ. Instrument calibration was carried out with standard silicon powder. Peaks were analyzed using Rigaku's PDXL software for phase identification and crystallite size calculation using the Scherrer equation. Scanning Electron Microscopy (SEM) imaging was performed using F E I Quanta FEG 200 to assess morphology and size distribution.

2.5. Analysis of the antioxidant activity of Ag nanoparticles.

Antioxidant activities were evaluated by five assays: DPPH (2,2-diphenyl-1-picryl-hydrazine), Superoxide Dismutase Radical Scavenging assay, $ABTS^+$ [2, 2-azino-bis-3-ethylbenzothiazoline-6-sulfonic acid], Ferric Reducing Antioxidant Potential (FRAP) assay, and Total Antioxidant Activity following Kourti [14] with slight modifications. Positive controls were ascorbic acid at 100 µg/mL for all assays. Methanol (for DPPH, ABTS, SOD, and total antioxidant) and distilled water (for FRAP) served as negative controls. For the DPPH assay, 0.1 mM DPPH in methanol was incubated with various nanoparticle concentrations for 30 minutes in the dark, and the absorbance was measured at 517 nm. For the SOD assay, the reaction mixtures were incubated with nanoparticles for 10 minutes, and the absorbance was recorded at 560 nm. The working solution for the ABTS assay was made by mixing 7 mM ABTS with 2.45 mM potassium persulfate and incubating for 10 minutes; the absorbance was measured at 734 nm. The FRAP assay involved mixing the nanoparticle samples with FRAP reagent, and after 30 minutes, absorbance at 593 nm was measured. The reagent solution was prepared, nanoparticles were mixed to varying concentrations, the mixture was incubated for 90 minutes, and absorbance was measured at 695 nm. All assays were performed in triplicate for accuracy.

2.6. Antibacterial activity.

The agar well diffusion method tested the antibacterial efficacy of algae-assisted AgNPs against Gram-positive (*Bacillus subtilis*, *Staphylococcus aureus* ATCC, *Staphylococcus aureus* MRSA) and Gram-negative (*Escherichia coli*, *Pseudomonas aeruginosa*) bacteria from Mahathi biotechnologies, Chennai. Nanoparticles (10 mg/mL) dissolved in distilled water were applied in 6 mm wells on Muller-Hinton agar inoculated to a McFarland standard of 1×10^6 CFU/mL. Plates were incubated at 37°C for 24 hours. Zones of inhibition (mm) were measured in triplicate. Results are expressed as mean ± standard deviation (SD). Statistical analysis was performed using one-way ANOVA. Amoxicillin (10µg/mL) served as a positive control, while $AgNO_3$ (1 mM) served as a negative control [15,16].

2.7. Cell viability assay.

The cell viability of the synthesized silver nanoparticles was evaluated using 3-(4,5-dimethylthiazol-2yl)-2,5-diphenyltetrazolium bromide (MTT) assay on human breast cancer cell lines (MCF-7). Cells were cultured in Dulbecco's Modified Eagle Medium (DMEM) incorporated with 10% fetal bovine serum (FBS), 1% penicillin-streptomycin, and maintained at 37°C in a humidified atmosphere containing 5% CO_2. Cells between passages 5 and 15 were used for all experiments to maintain consistency. After seeding in 96-well plates at a density of 1×10^4 cells/well and allowing 24 hours for attachment, the cells were treated with nanoparticle suspensions at concentrations ranging from 5 to 100 µg/mL for 24 hours [17]. MTT is cleaved by mitochondrial Succinate dehydrogenase and reductase of viable cells, yielding a measurable purple product formazan. Formazan formation reflects the number of metabolically active cells and decreases as cytotoxicity increases. After 48 h of incubation, MTT solution (5 mg/mL) was added to each well, and the plates were incubated for a further 2 h at room temperature. The medium was then carefully aspirated, 100 µL of DMSO was added to solubilize the formazan crystals, and the absorbance was measured at 570 nm using a Read Well Touch microplate reader [18]. All the experiments were performed in triplicate to ensure statistical validity.

Equation 2

$$Cell\ Viability\ =\ OD\ of\ Sample\ /\ OD\ of\ Control\ \times\ 100$$

3. Results and Discussion

One of the intriguing characteristics of this research is the synthesis of Ag nanoparticles mediated by the red algae *Gelidiella* sp. In this research, we have synthesized, characterized, and examined the potential applications in medicine. Our research has shown that antioxidant potential, along with antibacterial and cytotoxic properties, could aid in boosting anticancer drug efficacy [19].

3.1. Synthesis of nanoparticles.

The development of brown color in the reaction mixture suggests the formation of Ag nanoparticles. The color change of the reaction mixture indicates a reduction in metal ions and the formation of nanoparticles. A visible color change in the reaction mixture indicated the formation of silver nanoparticles, concurrent with the onset of the green reduction of silver

ions. This shift was evident when the algal extract turned light brown upon visual inspection. This alteration in color is primarily associated with bioactive constituents in the algae, which function as reducing, stabilizing, and capping agents for the nanoparticles. A visible color change in the reaction mixture indicated the formation of silver nanoparticles, concurrent with the onset of the green reduction of silver ions. This shift was evident when the algal extract turned light brown upon visual inspection [20]. This alteration in color is primarily associated with bioactive constituents in the algae, which function as reducing, stabilizing, and capping agents for the nanoparticles (Figure 1).

Figure 1. Visual observation of nanoparticle biosynthesis using *Gelidiella* sp. extract.

3.2. UV-vis analysis.

The UV-Vis absorption spectrum of *Gelidiella* sp. - mediated silver nanoparticles displayed a strong peak at 417 nm, characteristic of AgNPs due to their surface plasmon resonance (SPR) properties. The observed color change of the reaction mixture- from colorless to reddish brown- confirmed the reduction of $AgNO_3$ and successful nanoparticle formation. Although the peak at 417 nm confirms AgNP synthesis, this study did not include kinetic measurements to assess nanoparticle formation. The formation of the biosynthesized Silver NPs was confirmed by the absorption spectrum peak of Ag nanoparticles in the range of 350-480 nm due to their size-dependent optical properties [21]. After the reduction of NPs, the reaction mixture color also changed, which indicated the confirmation of the synthesis of NPs. The NPs showed a peak at 417 nm, and this characteristic absorbance peak confirmed that BNPs were successfully synthesized [Figure 2]. The increase in color intensity was positively associated with incubation duration. This enhancement is likely related to the excitation of the surface plasmon resonance (SPR) of the nanoparticles and the progressive reduction of AgNO3 by the algal extract [22-24].

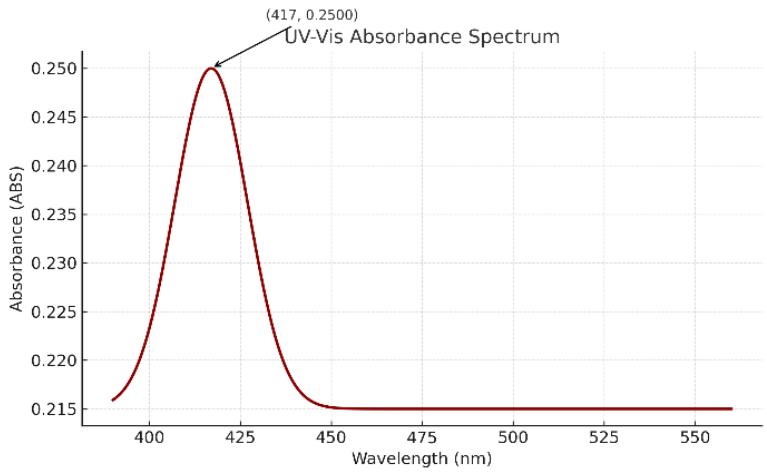

Figure 2. UV-visible spectrum of silver nanoparticles synthesized using *Gelidiella* sp. extract.

3.3. FTIR analysis.

FTIR spectra act as a tool for the determination of functional groups in the AgNPs. Figure 3 shows FT-IR spectra of the biosynthesized silver nanoparticles using *Gelidiella* sp. extract. The FTIR spectrum of NPs of *Gelidiella* sp. shows a broad peak around 3400 cm^{-1}, corresponding to O-H stretching vibrations, suggesting the presence of hydroxyl groups from alcohols or phenolic compounds. Peaks observed near 2920 cm^{-1} are associated with C-H stretching of aliphatic chains. A prominent band around 1640 cm^{-1} is attributed to C=O stretching (amide I), indicating the involvement of proteins in nanoparticle capping. The peaks in the region around 1400 cm^{-1} can be assigned to O-H bending or C-N stretching, further supporting the role of polyphenolic compounds and proteins. Additionally, strong absorption bands near 1100 cm^{-1} suggest C-O stretching vibrations, characteristic of alcohols, ethers, or polysaccharides. A weaker band near 600 cm-1 is attributed to metal-oxygen (Ag-O) bonding, confirming the interaction between silver and the biomolecules and indicating the formation of silver nanoparticles. This spectrum thus validates the role of *Gelidiella* sp. extract as both a reducing and stabilizing agent in the green synthesis of AgNPs. These verify that $AgNO_3$ nanoparticles were well integrated, as evidenced by the stable confirmation of the compounds. Concurrently, it was observed that absorption peak values differed among others [25-27].

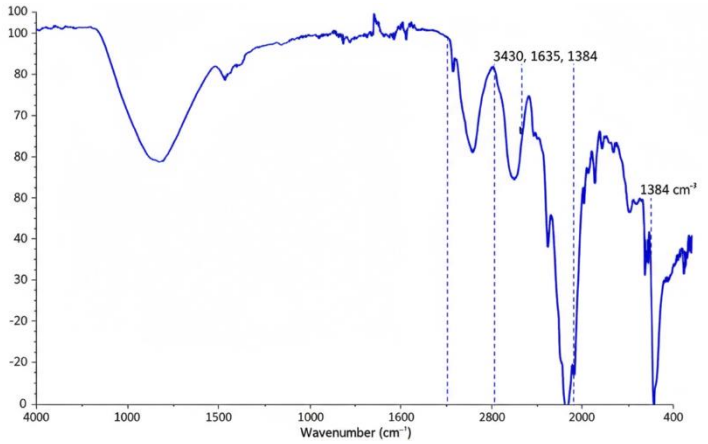

Figure 3. FTIR spectrum of *Gelidiella* sp. mediated silver nanoparticles.

3.4. XRD analysis.

The bio-synthesized nanoparticles (AgNPs) powder derived from *Gelidiella* sp., aqueous extracts exhibited XRD peaks, at approximately 2θ=38.2° (111), 44.3° (200), 64.5° (211), 79.6° (311) and, 83.3° (331), which correspond well with the JCPDS standard (No. 01-087-0718)for the cubic (face-centered cubic) structure of silver nitrate (Figure 8). These diffraction peaks confirmed the high purity of the synthesized material, as no impurity peaks were observed. The mean crystalline size of the AgNPs was calculated to be 58 nm using the Debye-Scherrer equation.

Equation 3

$$D = K\lambda/\beta cos\theta$$

Where D is the crystalline size, K is the shape factor (usually 0.9), λ is the X-ray wavelength (0.15406 nm for Cu K_α radiation), β is the full width at half maximum (FWHM) of the diffraction peak in radians, and θ is the Bragg angle. The FWHM was obtained from the prominent (111) peak in the XRD pattern, as shown in Figure 4. This calculation confirms the

nanoscale size and crystalline nature of the nanoparticles synthesized using the green method from *Gelidiella sp.* extract.

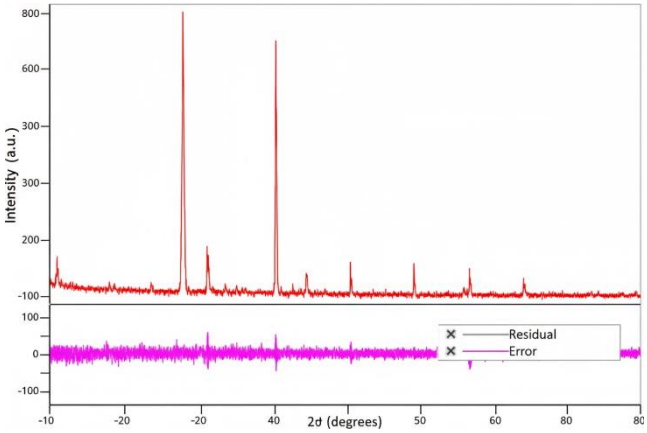

Figure 4. XRD pattern of synthesized *Gelidiella* sp. mediated silver nanoparticles.

3.5. SEM analysis.

The SEM analysis of silver nanoparticles biosynthesized using *the aqueous extract of Gelidiella sp. revealed high-density, relatively uniform nanoparticles with diameters of 50*-60 nm, consistent with XRD results. The nanoparticles were surrounded by bioorganic capping molecules, predominantly stabilized through hydrogen bonding and electrostatic interactions. However, the current SEM micrographs are due to hydrogen bonding and electrostatic interactions between the bioorganic capping molecules bound to the AgNPs. SEM analysis shows high-density AgNPs synthesized by the macroalgae *Gelidiella.* It was shown that relatively uniform AgNPs were formed with a diameter ranging from 50 to 60 nm, which coincides with the XRD results. Our results are in accordance with other reports on *Gelidiella* [28] AgNPs particle size [Figure 5a,b]. The findings of Jamil [29] SEM images of Fe-Ni bimetals revealed that the nanoparticles had merged surfaces, were irregular in form, ranged from 50-100 µm, and had a compact shape, which was uncertain and irregular [30].

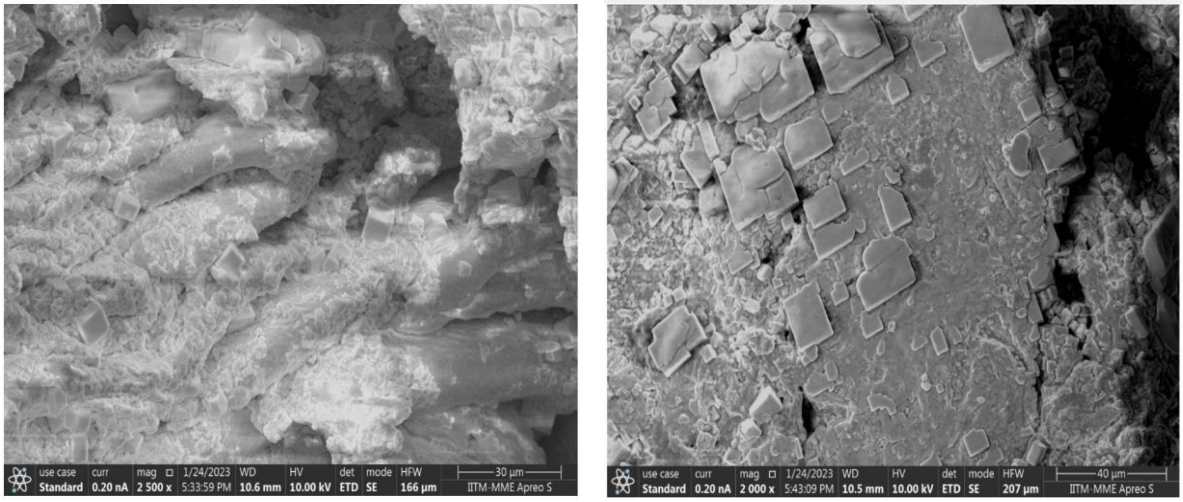

(a) **(b)**

Figure 5. SEM image of synthesized silver nanoparticles at different magnifications showing the surface morphology and particle distribution. **(a)** SEM image at 30 µm; **(b)** SEM image at 40 µm.

3.6. Antioxidant activity.

Five in vitro assays were used to assess the antioxidant activity of the algal extracts: DPPH (2,2-diphenyl-1-picryl-hydrazine) free radical scavenging assay, Superoxide Dismutase Radical Scavenging assay, $ABTS^{+}$ [2,2-azino-bis-3-ethylbenzothiazoline-6-sulfonic acid] Radical Cation Scavenging assay, Ferric Reducing Antioxidant Potential (FRAP) assay, and Total Antioxidant Activity [31,32]. Regression equations relating extract concentration to percentage inhibition were used to calculate IC50 values (the concentration required for 50% radical scavenging).

The IC_{50} values were calculated as 4.88, 7.0, 10.97, 17.42, and 5.5 µg/mL, respectively, for the assays (Figure 6a, b, c, d, and e). These antioxidant activities are likely due to bioactive compounds in *Gelidiella* sp., especially phenolics and flavonoids, which are known major contributors to antioxidant potential. A strong negative correlation typically exists between IC_{50} values and total phenolic/flavonoid content, indicating that higher phenolic content corresponds to more effective radical scavenging (lower IC_{50}).

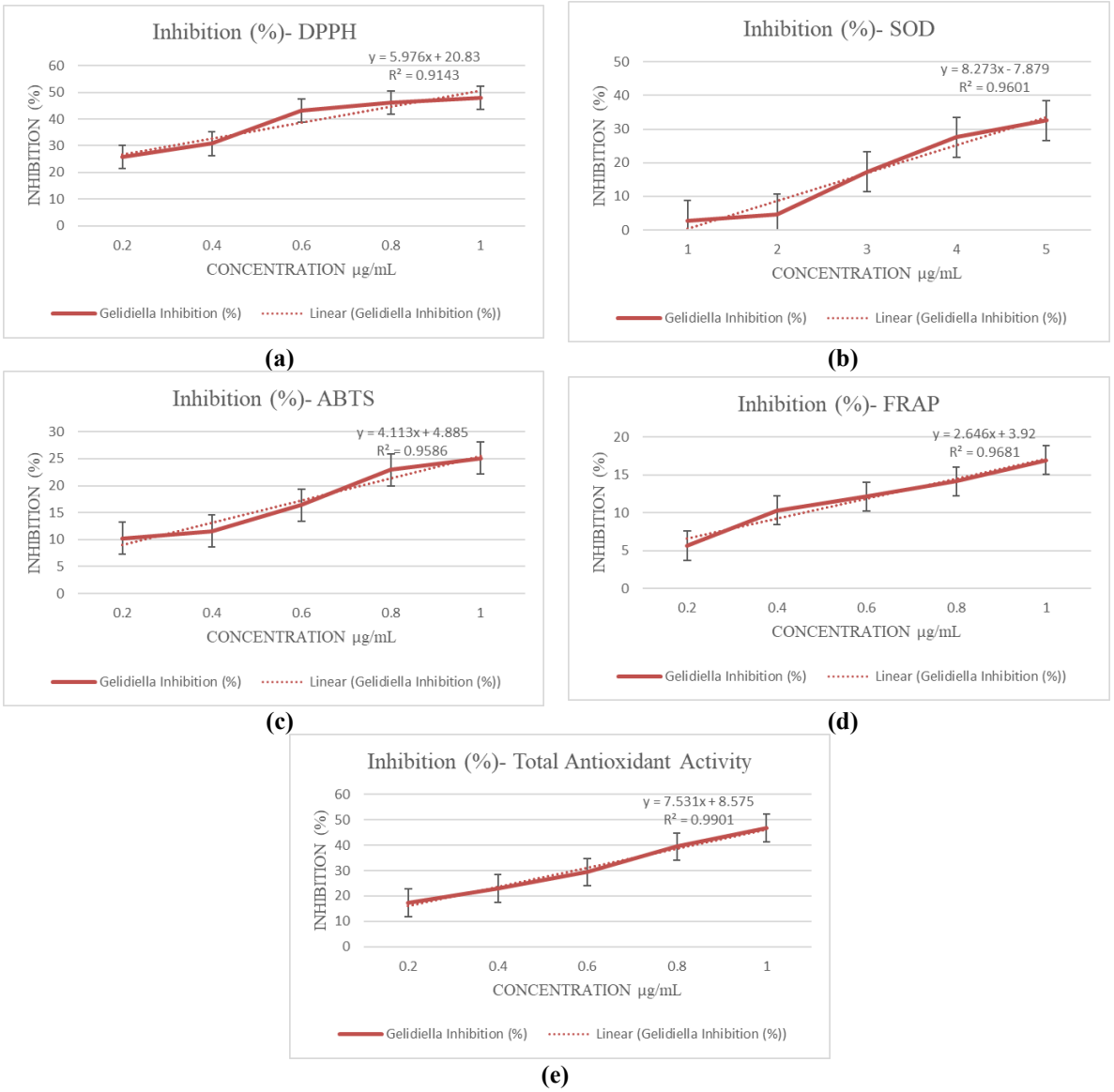

Figure 6. Antioxidant activity of the *Gelidiella* sp., mediated silver nanoparticles assessed by **(a)** DPPH; **(b)** SOD; **(c)** ABTS; **(d)** FRAP; **(e)** Total antioxidant activity. Error bars represent mean ± SD from three independent replicates (n=3).

Although specific phenolic and flavonoid contents were not quantified in this study, such correlations suggest the observed antioxidant efficacy stems largely from these compounds. The negative correlation between IC_{50} and total phenolic/flavonoid content strongly supports the mechanistic involvement of these bioactives. Further isolation and quantification of these bioactives could clarify their contributions and potentially improve nanoparticle antioxidant potency. Overall, the green-synthesized nanoparticles demonstrated potent antioxidant properties, comparable to or superior to those of standard antioxidants.

3.7. Antibacterial activity.

The synthesized silver nanoparticles (AgNPs) demonstrated antibacterial efficacy against both Gram-positive and Gram-negative bacterial strains, evaluated via the Mueller-Hinton agar well diffusion method. Silver nitrate solution served as the negative control, and amoxicillin as the positive control. At 100 µL concentration, the zone of inhibition for Gram-negative *Escherichia coli* and *Pseudomonas aeruginosa* was 23 and 24 mm, respectively, while for Gram-positive *Bacillus subtilis*, *Staphylococcus aureus*, *Staphylococcus aureus* ATCC, and *Staphylococcus aureus* MRSA, the zones were 21, 22, 22, and 20 mm, respectively (Figure 7, Table 1). *Pseudomonas aeruginosa* showed the highest sensitivity to the AgNPs. The differential susceptibility between Gram-negative and Gram-positive bacteria can be attributed to their distinct cell wall compositions. Gram-negative bacteria have an outer phospholipid permeability barrier, while Gram-positive bacteria possess a thick peptidoglycan layer without an outer membrane.

AgNPs exert their antibacterial effects through multiple mechanisms. Their nanoscale size and large surface area facilitate penetration and interaction with bacterial cell walls and membranes, resulting in physical membrane damage and rupture. Additionally, AgNPs induce the overproduction of reactive oxygen species (ROS), including hydroxyl radicals, superoxide anions, and hydrogen peroxide, leading to oxidative stress that damages lipids, proteins, and DNA within bacterial cells. This oxidative damage disrupts cellular respiration by inhibiting key respiratory enzymes, leading to energy depletion and cell death.

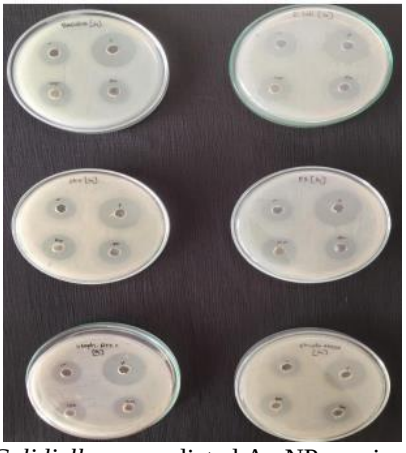

Figure 7. Antibacterial activity of *Gelidiella* sp. mediated Ag NPs against human pathogens. Six Petri dishes show zone of inhibition against (1) *Bacillus subtilis,* (2) *Escherichia coli,* (3) *Staphylococcus aureus,* (4) *Pseudomonas aeruginosa,* (5) *Staphylococcus aureus*- ATCC, and (6) *Staphylococcus aureus*- MRSA.

The generated ROS also impairs antioxidant enzyme activity, further exacerbating oxidative damage. AgNPs can interact with thiol groups in proteins, inactivating enzymatic functions crucial for bacterial survival, and can cause proton leakage through membranes,

resulting in loss of membrane potential and bacterial death. These multifaceted actions collectively contribute to the potent bactericidal activity observed, with a notable effect on Gram-negative bacteria likely due to differences in cell wall permeability and structure [33-35].

Table 1. Antibacterial activity of *Gelidiella* sp. mediated silver nanoparticles against human clinical pathogens**.**

Clinical pathogens	Positive control (mm)	Ag NPs (mm)	*Gelidiella* sp.		p value
			50 µL	100 µL	
Bacillus subtilis (+ve)	24 ± 0.5	20 ± 0.6	20 ± 0.4	21 ± 0.5	<0.05
Escherichia coli (-ve)	28 ± 0.4	21 ± 0.5	21 ± 0.3	**23 ± 0.6**	<0.01
Staphylococcus aureus (+ve)	26 ± 0.6	19 ± 0.4	21 ± 0.5	22 ± 0.4	<0.05
Pseudomonas aeruginosa (-ve)	28 ± 0.3	18 ± 0.5	21 ± 0.4	**24 ± 0.7**	<0.01
Staphylococcus aureus- ATCC (+ve)	29 ± 0.5	18 ± 0.6	21 ± 0.3	22 ± 0.5	<0.05
Staphylococcus aureus- MRSA (+ve)	26 ± 0.4	19 ± 0.4	18 ± 0.3	20 ± 0.4	<0.05

Values represent mean ± standard deviation (n=3). P-values were obtained using one-way ANOVA; $p<0.05$ was considered statistically significant.

3.8. Cell viability activity.

The cytotoxicity of *Gelidiella*-mediated silver nanoparticles (AgNPs) against MCF-7 breast cancer cells was assessed using the MTT assay, which showed a concentration-dependent decrease in cell viability with an IC_{50} of 94.41 µg/mL [Table 2]. At concentrations above 600 µg/mL, nearly complete death of cells was observed. These results are in alignment with other studies involving red and brown algae-derived AgNPs, supporting their pronounced anticancer activity (Figures 8a and 8 b) [36-39].

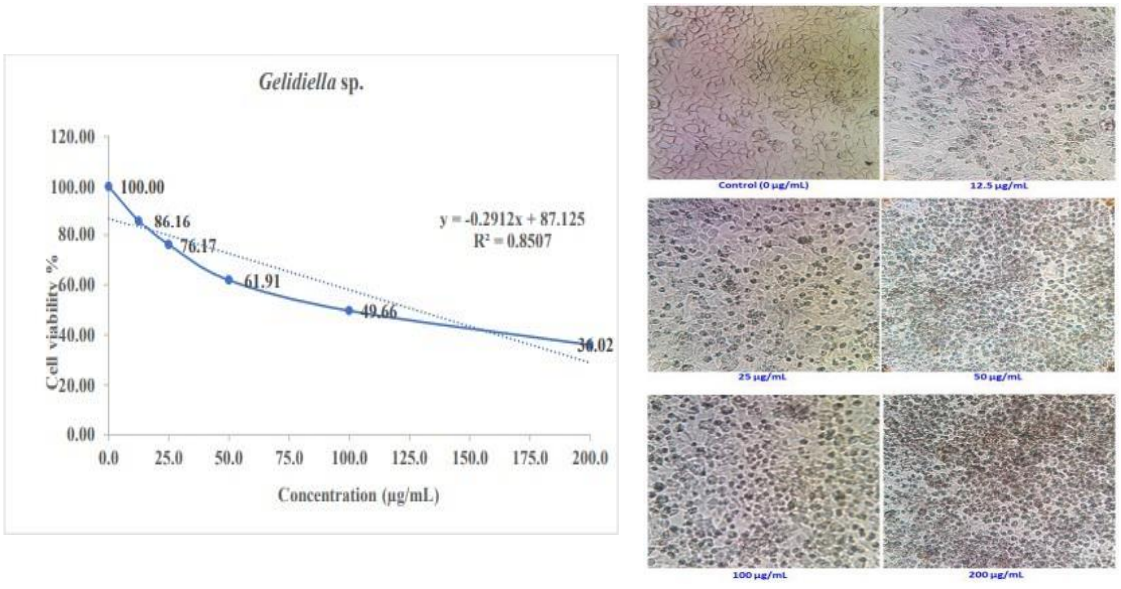

(a) **(b)**

Figure 8. (a) Cell viability; **(b)** Cytotoxicity effect of *Gelidiella* sp. mediated AgNPs against MCF-7 Cell lines. Error bars represent standard deviation (n=3).

The inhibition of MCF-7 cells by AgNPs is significantly influenced by particle size, charge, and surface chemistry. Nanoparticles sized 10-100 nm are most effective for anticancer delivery, as they are readily internalized via endocytosis, leading to higher local concentrations, extensive membrane interaction, and ROS generation. Smaller AgNPs (<20 nm) penetrate more deeply and induce greater DNA and mitochondrial disruption, while larger NPs (<30 nm), as in this study, maintain high uptake and retention within tumor cells. Surface charge (zeta potential) dictates cell-nanoparticle interaction. AgNPs with negative or neutral charge are

efficiently taken up by cells and demonstrate sufficient stability; highly negative charges can reduce uptake, whereas positive charges can enhance interaction with negatively charged cancer cell membranes. The *Gelidiella* extract provides bioactive capping agents-polysaccharides, phenolics- that influence surface chemistry, promote selective binding, and boost ROS generation within cancer cells, ultimately triggering apoptosis. The synergy of optimal size, favorable charge, and biofunctional surface chemistry explains the high cytotoxicity seen in *Gelidiella* AgNPs. This effect is potentiated by their ability to enhance oxidative stress, interfere with cell cycle control, promote membrane rupture, supporting their role as promising agents against breast cancer cells [40-43].

Table 2. *In vitro* cell viability of Gelidiella sp. mediated Ag NPs against MCF-7 cell lines.

Concentration (µg/mL)	Cell viability mean ± SD (%)	P value
0.0 (Control)	100.0 ± 0.00	-
12.5	86.16 ± 2.31	<0.05
25.0	76.17 ± 3.14	<0.01
50.0	61.91 ± 2.87	<0.001
100.0	49.66 ± 2.75	<0.001
200.0	30.02 ± 1.92	<0.001

Values represent the mean ± standard deviation of three independent experiments. Statistical significance was determined by one-way ANOVA compared to control (0.0 µg/mL); p-values <0.05 indicate significant cytotoxicity.

4. Conclusion

This study successfully demonstrates an environmentally friendly, low-cost green synthesis of silver nanoparticles (AgNPs) using *Gelidiella* sp., extract, yielding stable nanoparticles sized 50-60 nm, a UV-Vis absorption peak at 417 nm, and surface capping by bio-organic molecules such as amines, peptides, and secondary metabolites, as evidenced by FTIR analysis. These biomolecules facilitate extracellular bioreduction and confer nanoparticle stability in aqueous medium. These AgNPs exhibited strong antioxidant activity (IC50 values around 5 µg/mL) and potent antibacterial activity, achieving up to 24 mm inhibition zones against clinical pathogens. Cytotoxicity testing on MCF-7 breast cancer cells revealed an IC_{50} of 94.41 µg/mL, underscoring their biomedical potential. The physicochemical properties, such as nanoscale size, surface chemistry, and charge, play a crucial role in mediating these biological effects by enhancing cellular uptake, reactive oxygen species (ROS) generation, and molecular interaction with microbial and cancer cell membranes. Notably, this is the first report to correlate the physicochemical characteristics of Gelidiella sp.-derived AgNPs with their multifunctional bioactivities, advancing understanding of their mechanistic basis. Future work should focus on elucidating molecular mechanisms through advanced omics and imaging techniques, while validating in vivo efficacy and safety. Optimizing scalable, eco-friendly synthesis for targeted nanomedicine applications represents a promising translational path for these biogenic nanoparticles.

Author Contributions

Conceptualization, D.L. and A.S.P.; methodology, D.L.; validation, D.L.; formal analysis, D.L. and A.S.P.; investigation, D.L.; data curation, A.S.P.; writing—original draft preparation, D.L. and A.S.P.; writing—review and editing, A.S.P.; supervision, D.L. All authors have read and agreed to the published version of the manuscript.

Institutional Review Board Statement

Not applicable.

Informed Consent Statement

Not applicable.

Data Availability Statement

Data supporting the findings of this study are available upon reasonable request from the corresponding author.

Funding

This research was funded by the Management of SDNB Vaishnav College for Women, Chromepet, Chennai-44, India.

Acknowledgments

The authors are thankful to the management of SDNB Vaishnav College for Women, Chromepet, Chennai, Tamil Nadu, India, and Mahathi Biotechnologies, Ramapuram, Chennai-89, for providing the necessary facilities to carry out this study.

Conflicts of Interest

The authors declare no conflict of interest.

References

1. Ahmed, N.; Sheikh, M.A.; Ubaid, M.; Chauhan, P.; Kumar, K.; Choudhary, S. Comprehensive exploration of marine algae diversity, bioactive compounds, health benefits, regulatory issues, and food and drug applications. *Meas.: Food* **2024**, *14*, 100163, https://doi.org/10.1016/j.meafoo.2024.100163.
2. Eladl, S.N.; Elnabawy, A.M.; Eltanahy, E.G. Recent biotechnological applications of value-added bioactive compounds from microalgae and seaweeds. *Bot. Stud.* **2024**, *65*, 28, https://doi.org/10.1186/s40529-024-00434-y.
3. kazemi, S.; Hosseingholian, A.; Gohari, S.D.; Feirahi, F.; Moammeri, F.; Mesbahian, G.; Moghaddam, Z.S.; Ren, Q. Recent advances in green synthesized nanoparticles: from production to application. *Mater. Today Sustain.* **2023**, *24*, 100500, https://doi.org/10.1016/j.mtsust.2023.100500.
4. Osman, A.I.; Zhang, Y.; Farghali, M.; Rashwan, A.K.; Eltaweil, A.S.; Abd El-Monaem, E.M.; Mohamed, I.M.A.; Badr, M.M.; Ihara, I.; Rooney, D.W.; Yap, P.-S. Synthesis of green nanoparticles for energy, biomedical, environmental, agricultural, and food applications: A review. *Environ. Chem. Lett.* **2024**, *22*, 841-887, https://doi.org/10.1007/s10311-023-01682-3.
5. Nandhini, J.; Karthikeyan, E.; Rani, E.E.; Karthikha, V.S.; Sanjana, D.S.; Jeevitha, H.; Priyadharshan, A. Advancing engineered approaches for sustainable wound regeneration and repair: harnessing the potential of green synthesized silver nanoparticles. *Eng. Regener*. **2024**, *5*(3), 306-325, https://doi.org/10.1016/j.engreg.2024.06.004.
6. Mukherjee, S.; Verma, A.; Kong, L.; Rengan, A.K.; Cahill, D.M. Advancements in Green Nanoparticle Technology: Focusing on the Treatment of Clinical Phytopathogens. *Biomolecules* **2024**, *14*, 1082, https://doi.org/10.3390/biom14091082.
7. Vijayaram, S.; Razafindralambo, H.; Sun, Y.-Z.; Vasantharaj, S.; Ghafarifarsani, H.; Hoseinifar, S.H.; Raeeszadeh, M. Applications of Green Synthesized Metal Nanoparticles — a Review. *Biol. Trace Elem. Res.* **2024**, *202*, 360-386, https://doi.org/10.1007/s12011-023-03645-9.
8. Nabila, Z.; Ahmed, M.; Ayesha, K.; Taous, K.; Rozina, K.; Syeda Sohaila, N.; Fazli, W. Pharmaceutical

and Biomedical Applications of Green Synthesized Metal and Metal Oxide Nanoparticles. *Curr. Pharm. Des.* **2020**, *26*, 5844-5865, https://doi.org/10.2174/1381612826666201126144805.
9. Viswanathan, S.P.; Njazhakunnathu, G.V.; Neelamury, S.P.; Padmakumar, B.; Ambatt, T.P. The efficiency of aquatic weed–derived biochar in enhanced removal of cationic dyes from aqueous medium. *Biomass Conv. Bioref.* **2024**, *14*, 12895-12910, https://doi.org/10.1007/s13399-022-03546-2.
10. Vivek, M.; Kumar, P.S.; Steffi, S.; Sudha, S. Biogenic Silver Nanoparticles by Gelidiella acerosa Extract and their Antifungal Effects. *Avicenna J. Med. Biotechnol.* **2011**, *3*, 143-148.
11. Bourang, S.; Noruzpour, M.; Jahanbakhsh Godekahriz, S.; Ebrahimi, H.A.C.; Amani, A.; Asghari Zakaria, R.; Yaghoubi, H. Application of nanoparticles in breast cancer treatment: a systematic review. *Naunyn-Schmiedeberg's Arch. Pharmacol.* **2024**, *397*, 6459-6505, https://doi.org/10.1007/s00210-024-03082-y.
12. Chaudhari, R.; Patel, V.; Kumar, A. Cutting-edge approaches for targeted drug delivery in breast cancer: beyond conventional therapies. *Nanoscale Adv.* **2024**, *6*, 2270-2286, https://doi.org/10.1039/D4NA00086B.
13. Danbature, W.L.; Shehu, Z.; Yoro, M. Silver-Cobalt Bimetallic Nanoparticles as a Nanotechnological Method for Control of Culex quinquefasciatus-Borne Diseases. *Curr. Adv. Chem. Biochem.* **2021**, *1*, 1-9, https://doi.org/10.9734/bpi/cacb/v1/6999D.
14. Kourti, M.; Skaperda, Z.; Tekos, F.; Stathopoulos, P.; Koutra, C.; Skaltsounis, A.L.; Kouretas, D. The Bioactivity of a Hydroxytyrosol-Enriched Extract Originated after Direct Hydrolysis of Olive Leaves from Greek Cultivars. *Molecules* **2024**, *29*, 299, https://doi.org/10.3390/molecules29020299.
15. Papitha, A.S.; Lakshmi, D. Modelling and green synthesis of Ag–Co bimetallic nanoparticles using red alga (Gelidiella sp.) and their colloidal interaction with human pathogens. *Vegetos* **2025**, https://doi.org/10.1007/s42535-025-01442-4.
16. Sajidha Parveen, K.; Lakshmi, D. Biosynthesis of silver nanoparticles using red algae, *Amphiroa fragilissima* and its antibacterial potential against gram positive and gram negative bacteria. *Int. J. Curr. Sci.* **2016**, *19*, 93-100.
17. Gurunathan, S.; Park, J.H.; Han, J.W.; Kim, J.-H. Comparative assessment of the apoptotic potential of silver nanoparticles synthesized by *Bacillus tequilensis* and *Calocybe indica* in MDA-MB-231 human breast cancer cells: targeting p53 for anticancer therapy. *Int. J. Nanomed.* **2015**, *10*, 4203-4223, https://doi.org/10.2147/IJN.S83953.
18. Alinaghi, M.; Mokarram, P.; Ahmadi, M.; Bozorg-ghalati, F. Biosynthesis of palladium, platinum, and their bimetallic nanoparticles using rosemary and ginseng herbal plants: evaluation of anticancer activity. *Sci. Rep.* **2024**, *14*, 5798, https://doi.org/10.1038/s41598-024-56275-z.
19. Logeswari, V.; Yamini, S.; Pavithra, P.; Papitha, A.; Lakshmi, D. Study of Antioxidant, Antimicrobial and Cytotoxic Activities of Ag-Co Bimetallic Nanoparticles Biosynthesized from Red Alga (Amphiroa sp.). *Indian J. Sci. Technol* **2024**, *17*, 2013-2023, https://doi.org/10.17485/IJST/v17i19.861.
20. Thiurunavukkarau, R.; Shanmugam, S.; Subramanian, K.; Pandi, P.; Muralitharan, G.; Arokiarajan, M.; Kasinathan, K.; Sivaraj, A.; Kalyanasundaram, R.; AlOmar, S.Y.; Shanmugam, V. Silver nanoparticles synthesized from the seaweed Sargassum polycystum and screening for their biological potential. *Sci. Rep.* **2022**, *12*, 14757, https://doi.org/10.1038/s41598-022-18379-2.
21. Durán, L.; Castro, J.; Naranjo, J.; Fermín, J.R.; Rincón, C.A.D. Optical properties of $CuIn_5Se_8$ and $CuGa_5Se_8$ from ellipsometric measurements. *Mater. Chem. Phys.* **2009**, *114*, 73-77, https://doi.org/10.1016/j.matchemphys.2008.08.020.
22. Baker, C.; Pradhan, A.; Pakstis, L.; Pochan, D.J.; Shah, S.I. Synthesis and Antibacterial Properties of Silver Nanoparticles. *J. Nanosci. Nanotechnol.* **2005**, *5*, 244-249, https://doi.org/10.1166/jnn.2005.034.
23. Kathiraven, T.; Sundaramanickam, A.; Shanmugam, N.; Balasubramanian, T. Green synthesis of silver nanoparticles using marine algae Caulerpa racemosa and their antibacterial activity against some human pathogens. *Appl. Nanosci.* **2015**, *5*, 499-504, https://doi.org/10.1007/s13204-014-0341-2.
24. Nagarajan, S.; Arumugam Kuppusamy, K. Extracellular synthesis of zinc oxide nanoparticle using seaweeds of gulf of Mannar, *India*. *J. Nanobiotechnol.* **2013**, *11*, 39, https://doi.org/10.1186/1477-3155-11-39.
25. Kumar, P.; Senthamil Selvi, S.; Lakshmi Prabha, A.; Prem Kumar, K.; Ganeshkumar, R.S.; Govindaraju, M. Synthesis of silver nanoparticles from Sargassum tenerrimum and screening phytochemicals for its antibacterial activity. *Nano Biomed. Eng.* **2012**, *4*, 12-16, https://doi.org/10.5101/nbe.v4i1.p12-16.
26. Lengke, M.F.; Fleet, M.E.; Southam, G. Biosynthesis of Silver Nanoparticles by Filamentous Cyanobacteria from a Silver(I) Nitrate Complex. *Langmuir* **2007**, *23*, 2694-2699, https://doi.org/10.1021/la0613124.
27. McCord, J.M.; Fridovich, I. Superoxide Dismutase: AN ENZYMIC FUNCTION FOR ERYTHROCUPREIN (HEMOCUPREIN). *J. Biol. Chem.* **1969**, *244*, 6049-6055,

https://doi.org/10.1016/S0021-9258(18)63504-5.
28. Senthilkumar, P.; Surendran, L.; Sudhagar, B.; Ranjith Santhosh Kumar, D.S. Facile green synthesis of gold nanoparticles from marine algae *Gelidiella acerosa* and evaluation of its biological Potential. *SN Appl. Sci.* **2019**, *1*, 284, https://doi.org/10.1007/s42452-019-0284-z.
29. Jamil, S.; Khan, S.R.; Bibi, S.; Jahan, N.; Mushtaq, N.; Rafaqat, F.; Khan, R.A.; Gill, W.A.; Janjua, M.R.S.A. Recent advances in synthesis and characterization of iron–nickel bimetallic nanoparticles and their applications as photo-catalyst and fuel additive. *RSC Adv.* **2023**, *13*, 29632-29644, https://doi.org/10.1039/d3ra04293f.
30. Sharma, G.; Kumar, A.; Sharma, S.; Naushad, M.; Prakash Dwivedi, R.; Alothman, Z.A.; Mola, G.T. Novel development of nanoparticles to bimetallic nanoparticles and their composites: A review. *J. King Saud Univ. Sci.* **2019**, *31*, 257-269, https://doi.org/10.1016/j.jksus.2017.06.012.
31. Al-Radadi, N.S. Facile one-step green synthesis of gold nanoparticles (AuNp) using licorice root extract: Antimicrobial and anticancer study against HepG2 cell line. *Arab. J. Chem.* **2021**, *14*, 102956, https://doi.org/10.1016/j.arabjc.2020.102956.
32. Ansar, S.; Tabassum, H.; Aladwan, N.S.M.; Naiman Ali, M.; Almaarik, B.; AlMahrouqi, S.; Abudawood, M.; Banu, N.; Alsubki, R. Eco friendly silver nanoparticles synthesis by *Brassica oleracea* and its antibacterial, anticancer and antioxidant properties. *Sci. Rep.* **2020**, *10*, 18564, https://doi.org/10.1038/s41598-020-74371-8.
33. Chugh, D.; Viswamalya, V.S.; Das, B. Green synthesis of silver nanoparticles with algae and the importance of capping agents in the process. *J. Genet. Eng. Biotechnol.* **2021**, *19*, 126, https://doi.org/10.1186/s43141-021-00228-w.
34. Kannabiran, K.; Mohankumar, T.; Gunaseker, V. Evaluation of antimicrobial activity of saponin isolated from Solanum xanthocarpum and Centella asiatica. *Int. J. Nat. Eng. Sci*. **2009**, *3*(1), 22-25.
35. Perdikaki, A.; Galeou, A.; Pilatos, G.; Prombona, A.; Karanikolos, G.N. Ion-Based Metal/Graphene Antibacterial Agents Comprising Mono-Ionic and Bi-Ionic Silver and Copper Species. *Langmuir* **2018**, *34*, 11156-11166, https://doi.org/10.1021/acs.langmuir.8b01880.
36. Fatima, R.; Priya, M.; Indurthi, L.; Radhakrishnan, V.; Sudhakaran, R. Biosynthesis of silver nanoparticles using red algae *Portieria hornemannii* and its antibacterial activity against fish pathogens. *Microb. Pathog.* **2020**, *138*, 103780, https://doi.org/10.1016/j.micpath.2019.103780.
37. Suganya, S.; Dhanalakshmi, B.; Dinesh Kumar, S.; Santhanam, P. Cytotoxic Effect of Silver Nanoparticles Synthesized from Sargassum wightii on Cervical Cancer Cell Line. *Proc. Natl. Acad. Sci., India, Sect. B Biol. Sci.* **2020**, *90*, 811-818, https://doi.org/10.1007/s40011-019-01152-3.
38. Viswanathan, S.; Palaniyandi, T.; Shanmugam, R.; Karunakaran, S.; Pandi, M.; Wahab, M.R.A.; Baskar, G.; Rajendran, B.K.; Sivaji, A.; Moovendhan, M. Synthesis, characterization, cytotoxicity, and antimicrobial studies of green synthesized silver nanoparticles using red seaweed *Champia parvula*. *Biomass Conv. Bioref.* **2024**, *14*, 7387-7400, https://doi.org/10.1007/s13399-023-03775-z.
39. Khalaf, W.Y.; Elias, R.S.; Raheem, L.A. Design, synthesis and molecular docking study of coumarin pyrazoline derivatives against MCF-7 breast cancer cell line. *Pharmacia* **2023**, *70*, 1487-1492, https://doi.org/10.3897/pharmacia.70.e108670.
40. Khorrami, S.; Zarrabi, A.; Khaleghi, M.; Danaei, M.; Mozafari, M.R. Selective cytotoxicity of green synthesized silver nanoparticles against the MCF-7 tumor cell line and their enhanced antioxidant and antimicrobial properties. *Int. J. Nanomed.* **2018**, *13*, 8013-8024, https://doi.org/10.2147/IJN.S189295.
41. Akter, M.; Sikder, M.T.; Rahman, M.M.; Ullah, A.K.M.A.; Hossain, K.F.B.; Banik, S.; Hosokawa, T.; Saito, T.; Kurasaki, M. A systematic review on silver nanoparticles-induced cytotoxicity: Physicochemical properties and perspectives. *J. Adv. Res.* **2018**, *9*, 1-16, https://doi.org/10.1016/j.jare.2017.10.008.
42. Pucelik, B.; Sułek, A.; Borkowski, M.; Barzowska, A.; Kobielusz, M.; Dąbrowski, J.M. Synthesis and Characterization of Size- and Charge-Tunable Silver Nanoparticles for Selective Anticancer and Antibacterial Treatment. *ACS Appl. Mater. Interfaces* **2022**, *14*, 14981-14996, https://doi.org/10.1021/acsami.2c01100.
43. Madaniyah, L.; Fiddaroini, S.; Hayati, E.K.; Rahman, M.F.; Sabarudin, A. Biosynthesis, characterization, and in-vitro anticancer effect of plant-mediated silver nanoparticles using *Acalypha indica Linn*: In-silico approach. *OpenNano* **2025**, *21*, 100220, https://doi.org/10.1016/j.onano.2024.100220.

Publisher's Note & Disclaimer